HAL
open science

Ultrasound contrast agents modeling using an extended Volterra model

Fatima Sbeity, Jean-Marc Girault, Sébastien Ménigot, Jamal Charara

To cite this version:

Fatima Sbeity, Jean-Marc Girault, Sébastien Ménigot, Jamal Charara. Ultrasound contrast agents modeling using an extended Volterra model. Acoustics 2012, Apr 2012, Nantes, France. hal-00810770

HAL Id: hal-00810770

https://hal.science/hal-00810770v1

Submitted on 23 Apr 2012

HAL is a multi-disciplinary open access archive for the deposit and dissemination of scientific research documents, whether they are published or not. The documents may come from teaching and research institutions in France or abroad, or from public or private research centers.

L'archive ouverte pluridisciplinaire **HAL**, est destinée au dépôt et à la diffusion de documents scientifiques de niveau recherche, publiés ou non, émanant des établissements d'enseignement et de recherche français ou étrangers, des laboratoires publics ou privés.

Ultrasound contrast agents modeling using an extended Volterra model

F. Sbeity[a], J.-M. Girault[a], S. Ménigot[a] and J. Charara[b]

[a]Imagerie et cerveau, Hôpital Bretonneau 1 Bd Tonnelle 37044 Tours
[b]Université Libanaise,
fatima.sbeity@etu.univ-tours.fr

Harmonic imaging has historically occurred with the introduction of ultrasound contrast agents such as microbubbles. These agents, due to their nonlinear behavior, have provided a great increase in the contrast of ultrasound images. Although this modality has revolutionized the clinical practice, it still suffers from the presence of harmonics in the echo of the tissue that reduces its efficiency. One way to overcome this problem was to turn to the sub- and ultra-harmonic imaging based on the reception of sub-harmonics ($\frac{1}{2}f_0$) and ultra-harmonics ($\frac{3}{2}f_0, \frac{5}{2}f_0, ...$) generated by the microbubbles at high pressure levels. Nonlinear existing models like Volterra series are able to model harmonics only. In this paper, we proposed an extended Volterra model able to model and extract these sub- and ultra-harmonics. Results showed that sub- and ultra-harmonics were extracted and separated from other harmonic components. Signals backscattered by the medium infused with microbubbles can be accurately represented by the derived model. The gain achieved with our method was 3.7 dB compared to the standard Volterra modeling. In the frequency domain, the spectrum of the simulated signal has described perfectly that of the microbubble.

1 Introduction

The diagnostic capabilities of ultrasound imaging have been greatly improved by the intravenous injection of ultrasound contrast agents such as microbubbles [1]. This contrast enhancement is due to two principal reasons. From one hand side, the acoustic impedance of microbubbles is largely different than that of tissues [2, 3] and, from the other side, the response of microbubbles is nonlinear [2, 4]. This non linearity is directly observable through the presence of harmonics that can be extracted by filtering [5]. For instance, in second harmonic imaging, the principle is to excite the medium at a frequency f_0 and to reconstruct the image at the first harmonic *i.e.* around $2f_0$ [5, 6]. However, the generation of nonlinear components during the propagation in tissue limits the contrast. These nonlinear components can be reduced in part by reducing the emitting pressure [5, 6, 7, 8]. One alternative solution to distinguish microbubbles from surrounding tissue is to use the difference in signatures between the two media through sub- and ultra-harmonic imaging. Unlike tissues, experimental studies have shown the existence of sub- and ultra-harmonics in the response of microbbubles [1, 6, 8, 9]. In ultrasound contrast imaging, subharmonic imaging consists of emitting at a frequency f_0 and receiving at the sub-harmonic $\frac{f_0}{2}$ while ultraharmonic imaging is based on the reception of ($\frac{3}{2}f_0, \frac{5}{2}f_0, ...$). Many in vitro studies showed the possibility of the application of subharmonic imaging in early detection of the angiogenesis around tumors [3]. The reception of sub-harmonics may be done using a narrow band transducer for the reception with center frequency $\frac{1}{2}f_0$[3, 10].

In order to improve the image contrast, it is necessary to understand the behavior of microbubbles. Indeed, the dynamics of the microbubble is quite well understood and many nonlinear models have been proposed [2]. Various modifications were performed to accommodate the microbubble shell and the nonlinearities, including the Rayleigh-Plesset modified equation [11, 12, 13].

Although these models accurately simulate the oscillation of microbubbles, other models that consider the system to be studied as a black box, have been used to optimally model microbubbles signals. The best known one is the Volterra series which has a capacity to describe the input-output behavior of nonlinear dynamic systems [14]. Volterra series have already been employed in ultrasound contrast imaging and contributed to increase the contrast of images [15]. These series, that are able to model and extract the harmonic components only [14], are power series of integer orders. However, there is no simple mathematical model able to extract sub- and ultra-harmonics from microbubbles signals. However the modeling of sub-harmonics using Multiple Input Single Output (MISO) Volterra series is discussed in [16]. This approach is unable to extract these components and separate them from other components.

We proposed in this study an original solution based on the Volterra series that enabled to model and extract sub- and ultra-harmonic components. The originality in this work resided in the simplicity of the proposed method that used existing mathematical operators.

2 Materials and Method

The purpose of our dissertation was to develop a Volterra series based model to model microbubbles signals in presence of sub- and ultra-harmonics of order $\frac{1}{2}$ ($f_n = \frac{n}{2}f_0$, where n is an odd integer) and to extract them. The nonlinear system to be identified was the microbubble excited by a pressure wave $x(n)$ (the input signal). By solving numerically the nonlinear differential equation of a microbubble, subjected to a pressure signal, the backscattered signal by the microbubbles $y(n)$ (the output signal) was obtained (see Figure 1).

The dynamics of a microbubble were simulated by solving the Rayleigh-Plesset modified equation using Hoff's method [11]. The incident wave to the microbubble was a sinusoidal signal apodized with Hanning window, of frequency f_0 = 4 MHz, 1.6 MPa pressure, and 32 cycles. Under the previous frequency and pressure conditions, the oscillation of the microbubble is nonlinear including sub- and ultra-harmonics [8]. The backscattered signal was sampled f_s = 36 MHz. The parameters of microbubbles are shown in table 1.

Table 1: Parameters of microbubbles [11].

resting radius	$r_0 = 2\mu m$
shell thickness	$d_{Se} = 4nm$
shear modulus	$G_s = 50MPa$
shear viscosity	$\eta = 0.8Pa.s$

2.1 Volterra model

The Volterra model is equivalent to a power series decomposition of integer orders. To model and extract the sub- and ultra-harmonic frequencies, we proposed to extend the standard Volterra series by adding a component dedicated to them.

Volterra series were introduced as Taylor series with memory. Let $y(n)$ be the scattered signal by the medium infused with microbubbles. The output $y(n)$ can be expressed in terms of the present and previous inputs $x(n)$ and $x(n-k)$, respectively. The general form of the Volterra model $(3, m)$, of order 3 and memory m, in the discrete time was as follows [17]:

$$\begin{aligned}\hat{y}(n) &= h_0 + \sum_{k_1=0}^{m-1} h_1(k_1)x(n-k_1) \\ &+ \sum_{k_1=0}^{m-1}\sum_{k_2=0}^{m-1} h_2(k_1,k_2)x(n-k_1)x(n-k_2) \\ &+ \sum_{k_1=0}^{m-1}\sum_{k_2=0}^{m-1}\sum_{k_3=0}^{m-1} h_3(k_1,k_2,k_3)x(n-k_1)x(n-k_2)x(n-k_3).\end{aligned} \tag{1}$$

where $\hat{y}(n)$ was the observed output sequence associated with the input sequence $x(n)$, and $h_p(k_1, k_2, \ldots, k_p)$ were the Volterra kernels of order p of the development. The order 3 of the Volterra series is sufficient given the limited bandwidth of ultrasound transducers [14]. If the function V_H^m were the Volterra model, $\hat{y}_H(n)$ could be expressed as:

$$\hat{y}_H(n) = V_H^m(x(n)). \tag{2}$$

The Volterra's coefficients $h_p(k_1, k_2, \ldots, k_p)$ were obtained by minimizing the mean square error between the two signals $y(n)$ and $\hat{y}_H(n)$ (Figure 1):

$$\arg\min[(y(n) - \hat{y}_H(n))^2]. \tag{3}$$

The calculation method was similar to that developed by [14] but without the Cholesky decomposition.

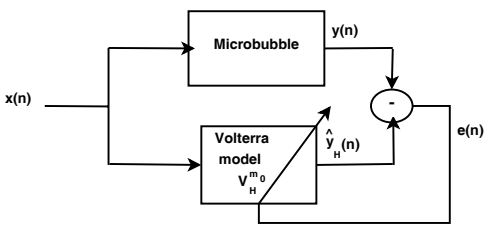

Figure 1: Identification of the nonlinear system of the microbubble with the Volterra model.

2.2 Extended Volterra model

The extended Volterra model that we proposed, allowed identifying the harmonic, sub-harmonic, and ultra-harmonic components. The corresponding output sequence of our extended Volterra model could be written as follows:

$$\hat{y}(n) = V_{SUH}^m(x(n)). \tag{4}$$

The solution that we proposed consisted of two parts:

$$V_{SUH}^m(x(n)) = V_H^m(x(n)) + V_{SU}^m(x(n)). \tag{5}$$

A part that modeled exclusively the harmonics:

$$\hat{y}_H(n) = V_H^m(x(n)), \tag{6}$$

and another that modeled the sub- and ultra-harmonics:

$$\hat{y}_{SU}(n) = V_{SU}^m(x(n)). \tag{7}$$

The reconstructed signal of the microbubble was then:

$$\hat{y}(n) = \hat{y}_H(n) + \hat{y}_{SU}(n). \tag{8}$$

2.3 Numerical procedure

The numerical procedure was written with Matlab (Mathworks, Natick, MA, USA). It included the following steps:

1. Modeling of integer harmonics: it was the Volterra model $(3, m)$. The obtained signal was given by equation (6);

2. Modeling of sub- and ultra-harmonics of order $\frac{1}{2}$:

   (a) The analytic signal $y_a(n)$, whose spectrum contained only positive frequencies was modulated by multiplying it by an exponential having a frequency $\frac{1}{2}f_0$. The modulated signal was then:

   $$y_{a_{mod}}(n) = y_a(n)e^{(2j\pi\frac{f_0}{2}n)}, \tag{9}$$

   with:

   $$y_a(n) = y(n) + jH(y(n)), \tag{10}$$

   where $H(y(n))$ was the Hilbert transform of $y(n)$. From a spectral point of view, the modulation shifted the spectrum by $\frac{1}{2}f_0$. Indeed, if the spectrum of $y(n)$ included $\frac{1}{2}f_0$ and f_0 components, then the spectrum of $y_{a_{mod}}$ will be composed of $f_0 = (\frac{1}{2}f_0 + \frac{1}{2}f_0)$ and $\frac{3}{2}f_0 = (f_0 + \frac{1}{2}f_0)$ components. The signal $y_{a_{mod}}$ contained shifted sub- and ultra-harmonics instead of harmonics.

   (b) A Volterra model of order $(3, m)$ identified the real part of the modulated signal $R(y_{a_{mod}}(n))$ by minimizing the following relation:

   $$\arg\min[(R(y_{a_{mod}}(n)) - \hat{y}_2(n))^2]. \tag{11}$$

   The Volterra model extracted the harmonic components around nf_0 (n is an integer) which were initially the sub- and ultra-components. The modeled signal became:

   $$\hat{y}_2(n) = V_H^m(x(n)). \tag{12}$$

   (c) The analytic signal $\hat{y}_{2_a}(n)$ was demodulated with a frequency $(-\frac{1}{2}f_0)$, that shifted the harmonic components as well as the sub- and ultra-harmonic components back to their original positions.
   The demodulated signal became:

   $$\hat{y}_{2_{a_{demod}}}(n) = \hat{y}_{2_a}(n)e^{(-2j\pi\frac{f_0}{2}n)}. \tag{13}$$

   The double application of the Hilbert transform introduced a negative sign. For this reason, we multiplied the demodulated signal by $e^{j\pi}$. In order to obtain the positive and negative frequencies of the demodulated signal we considered its real part merely. We obtained:

   $$\hat{y}_{SU}(n) = R(\hat{y}_{2_{a_{demod}}}(n))e^{j\pi} = -R(\hat{y}_{2_{a_{demod}}}(n)). \tag{14}$$

The final modeled signal $\hat{y}(n)$ was obtained by adding the two signals $\hat{y}_H(n)$ and $\hat{y}_{SU}(n)$ as given by equation (8). The extended Volterra model was symbolized by $(3, \frac{1}{2}, m)$ where 3 is the model order, $\frac{1}{2}$ is the coefficient of modulation and m is the model memory. Figure 2 showed the different steps

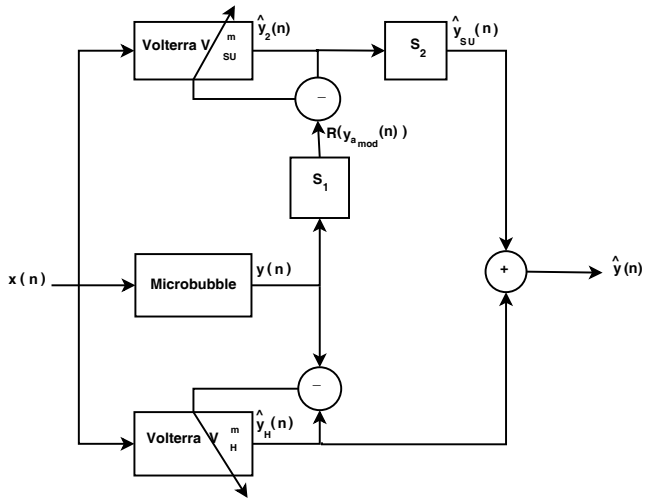

Figure 2: Blockdiagram of the extended volterra model $(3, \frac{1}{2}, m)$.

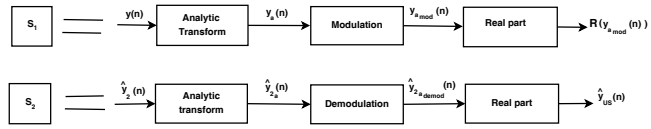

Figure 3: Blockdiagram of the two systems S_1 et S_2.

of the extended Volterra model while figure 3 showed both systems S_1 and S_2 .

The relative mean square error *RMSE* used to evaluate the accuracy of our method was given by:

$$RMSE = \frac{|\hat{y}(n) - y(n)|^2}{|y(n)|^2}, \tag{15}$$

where $\hat{y}(n)$ was the final signal reconstructed by the extended Volterra model and $y(n)$ was the signal backscattered by the microbubble.

3 Results

To verify the efficiency of our method, we applied both the Volterra model $(3, 4)$ as well as the extended Volterra model $(3, \frac{1}{2}, 4)$ to a synthetic microbubble signal. The microbubble was insonified with the sine pulse described in section 2 et the backscattered signal was then calculated.

Qualitatively, Figure 4(a) shows the backscattered signal $y(n)$ and that modeled by the extended Volterra model $(3, \frac{1}{2}, 4)$ $\hat{y}(n)$ versus time. Figure 4(b) shows the difference between $y(n)$ and $\hat{y}(n)$. Figure 4(c) shows the harmonic signal $\hat{y}_H(n)$ obtained with the standard model $(3, 4)$, and figure 4(d) shows the sub- and ultra-harmonic signal $\hat{y}_{SU}(n)$ extracted with the extended model $(3, \frac{1}{2}, 4)$.

Figure 5 shows the spectra of the various signals shown in figure 4. The spectral composition of these signals was in good qualitative agreement with figure 4. These figures show that sub- and ultra-harmonics components were modeled, extracted and separated from other harmonic components.

Quantitatively, table 2 shows a comparison of the *RMSE* between the the signal modeled with the extended model and that modeled with the standard model. The gain achieved was 3.7 dB (the difference between *RMSE* between the reconstructed signal with the extended Volterra model and the

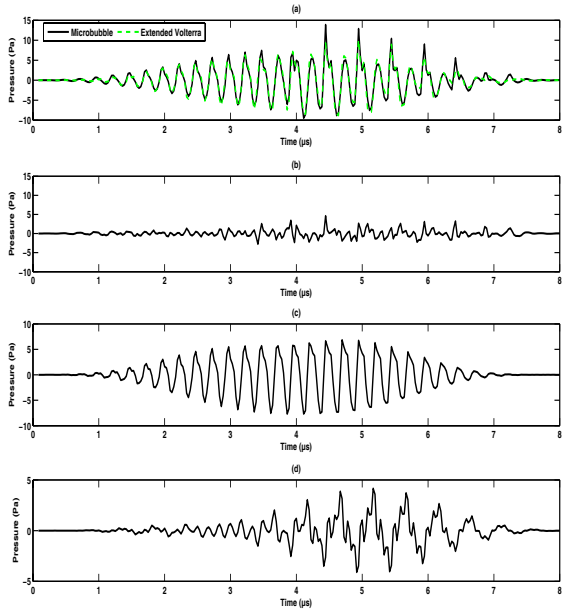

Figure 4: (a) Backscattered signal $y(n)$ by the microbubble and the reconstructed signal $\hat{y}(n)$ by the extended Volterra model of order $(3, \frac{1}{2}, 4)$. (b) Error signal between $y(n)$ and $\hat{y}(n)$. (c) Harmonic signal $\hat{y}_H(n)$. (d) Sub- and ultra-harmonic signal $\hat{y}_{SU}(n)$.

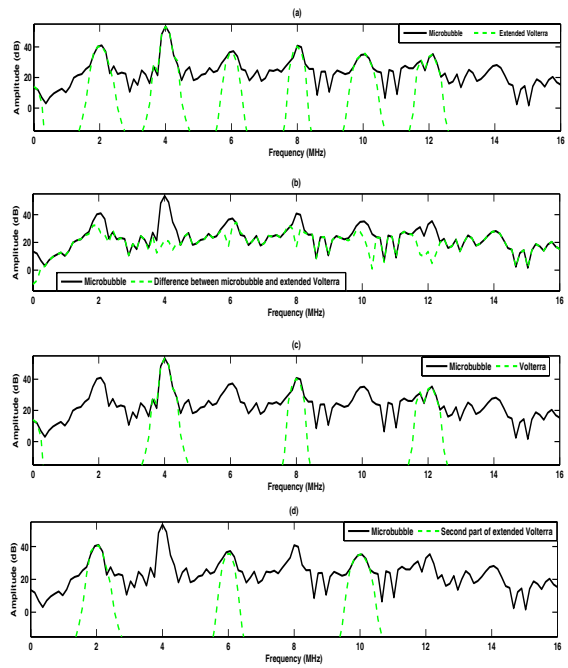

Figure 5: (a) Spectrum of the microbubble signal $y(n)$ and the reconstructed signal $\hat{y}(n)$ by the extended Volterra model $(3, \frac{1}{2}, 4)$. (b) Spectrum of the error signal between $y(n)$ and $\hat{y}(n)$. (c) Harmonic spectrum $\hat{Y}_H(f)$. (d) Sub- and ultra-harmonic spectrum $\hat{Y}_{SU}(f)$.

backscattered signal (-11.5) dB and the *RMSE* between the reconstructed signal with the standard Volterra model and the backscattered signal (-7.8) dB with the application of the extended Volterra model).

Table 2: Relative mean square errors *RMSE* (dB) between the signal backscattered by the microbubble and that modeled with the Volterra model $(3, 4)$, and between the signal backscattered by the microbubble and that modeled with the extended Volterra model $(3, \frac{1}{2}, 4)$.

Model	Standard Volterra	extended Volterra
RMSE (dB)	−7.8	−11.5

4 Discussion

The ultrasound contrast agents promoted the generation of sub- and ultra-harmonics that did not show up in the echo of tissues. The application of the extended Volterra model on simulated signals of microbubbles showed a high efficiency to extract and recover sub- and ultra-harmonics of order $\frac{1}{2}$: $f_n = \frac{n}{2} f_0$ apart of harmonics. This result overcame the weakness of the standard Volterra model which modeled harmonics only. Extracted sub- and ultra-harmonics could be used to make sub- and ultraharmonic contrast imaging in order to produce high contrat images.

In addition, the extended model modeled the microbubble signal with a gain 3.7 dB compared to the standard Volterra model. In the frequency domain, all the frequency components of the backsacttered signal were correctly reconstructed. The identification process of the parameters enabled modeling of signals even at very high excitation pressure (1.6 MPa) known to exhibit sub-harmonics.

5 Conclusion

In our dissertation, we proposed an extended Volterra model. The originality of this model lied in enabling the extraction of sub- and ultra-harmonics components of microbubbles signals. In addition, modeling the microbubble signal, may be performed even at high pressure levels, unlike the standard Volterra model.

This method enabled the separation of sub- and ultra-harmo-nics components. Such tool could be greatly effective in the field of ultrasound contrast imaging. Especially the sub- and ultra-hamronic contrast imaging.

This work could be able to complete by calculating the parameters of sub- and ultra-harmonics in order to separate them, and developing an automatic method to calculate the contrast-to-tissue ratio (CTR) using these parameters.

Acknowledgements

The authors would to thank the Lebanese council of scientific research (CNRSL) for financing support.

References

[1] W.T. Shi, F. Forsberg, J.S. Raichlen, L. Needleman, and B. B. Goldberg, " subharmonic imaging of contrast agents ", *Ultrasound Med Biol* **25**, 275-283 (1999).

[2] T.G. eighton, The acoustic bubble, *Academic Press, London, UK,* (1994).

[3] G. Bhagavatheeshwaran, W.T. Shi, F. Forsberg, P.M. Shankar, "Subharmonic signal generation from contrast agents in simulated neovessels", *Ultrasound Med Biol* **30**, 199-203 (2004).

[4] S. Qin, K. W. Ferrara, "The natural frequency of nonlinear oscillation of ultrasound contrast agents in microvessels", *Ultrasound Med Biol* **33**, 1140-1148 (2007).

[5] C. Kollmann, "New xonographic techniques for harmonic imaging underlying physical principles", *Eur J Radiol* **64**, 164-172 (2007).

[6] P. M. Shankar, P.D. Krishna, V.L. Newhouse, "Advantages of subharmonic over second harmonic backscatter for Contrast-To-Tissue echo enhancement", *Ultrasound Med Biol* **24**, 395-399 (1998).

[7] M. Averkiou, "Tissue Harmonic Imaging", **2**, 1563-1572(2000).

[8] F. Forsberg, W.T. Shi, B.B. Goldberg, "Subharmonic imaging of contrast agents", *Ultrasonics* **38**, 93-98 (2000).

[9] R. Basude, M.A. Wheatley, "Generation of ultraharmonics in surfactant based ultrasound contrast agents: use and advantages", *Ultrasonics* **39**, 437-444 (2001).

[10] J.R. Eisenbrey, J.K. Dave, V.G. Halldorsdottir, D.A. Merton, P. Machado, J.B. Liu, C. Miller, J.M. Gonzalez, S. Park, S. Dianis, C.I. Chalek, K.E. Thomenius, D.B. Brown, V. Navarro, F.O. Forsberg, "Simultaneous grayscale and subharmonic ultrasound imaging on a modified commercial scanner", *Ultrasonics* **51**,890-897 (2003).

[11] L. Hoff, "Acoustic characterization of contrast agents for medical ultrasound imaging", *Kluwer Academic, Boston, USA*, (2001).

[12] K. E. Morgan, J. S. Allen, P. A. Dayton, J.E. Chomas, A. L. Klibaov, K. W. Ferrara, "Experimental and theoretical evaluation of microbubble behavior: Effect of transmitted phase and bubble size", *IEEE T Ultrason Ferr* **47**, 1494-1509 (2000).

[13] P. Marmottant, S. van der Meer, M. Emmer, M. Versluis, N. de Jong, S. Hilgenfeldt, and D. Lohse, "A model for large amplitude oscillations of coated bubbles accounting for buckling and rupture", *J Acoust Soc Am* **118**,3499-3505(2005).

[14] M. Mleczko, M. Postema, G. Schmitz, "Discussion of the application of finite Volterra series for the modeling of the oscillation behavior of ultrasound contrast agents", *Appl Acoust* **70**, 1363-1369 (2009).

[15] P. Phukpattaranont, E. S. Ebbini, "Post-beamforming second-order Volterra filter for pulse-echo ultrasonic imaging",*IEEE T Ultrason Ferr* **50**,987-1001(2003).

[16] O. Boaghe, S. Billings,"Subharmonic oscillation modeling and MISO Volterra series", *IEEE Transactions On Circuits And Systems* **50**,877-884 (2003).

[17] A.S. Soni, ”Control-relevant system identification using nonlinear Volterra and Volterra-Laguerre models”, PhD thesis, University of Pittsburgh, Pittsburgh, PA, USA, 2006.